PCCP

Accepted Manuscript

ROYAL SOCIETY OF CHEMISTRY

www.rsc.org/pccp

CREATED USING THE RSC LaTeX PCCP ARTICLE TEMPLATE – SEE www.rsc.org/electronicfiles FOR DETAILS

ARTICLE TYPE www. rsc.org/xxxxxx | XXXXXXXX

C_{60} Molecules grown on a Si-supported Nanoporous Supramolecular Network: a DFT study

Khaoula Boukari,[a] Eric Duverger,[b] Régis Stephan,[a] Marie-Christine Hanf,*[a] and Philippe Sonnet[a]

Received Xth XXXXXXXXXX 20XX, Accepted Xth XXXXXXXXX 20XX

First published on the web Xth XXXXXXXXXX 200X

DOI: 10.1039/b000000x

C_{60} fullerene assemblies on surfaces have attracted considerable attention because of their remarkable electronic properties. Now because of the competition between the molecules-substrate and the molecule-molecule interactions, an ordered C_{60} array is rather difficult to obtain on silicon surfaces. Here we present density functional theory simulations on C_{60} molecules deposited on a TBB (1,3,5-tri(1'-bromophenyl)benzene) monolayer lying on the Si(111)-boron surface (denoted SiB). The C_{60} molecules are located in the nanopores formed by the TBB network. Adsorption energy calculations show that the SiB surface governs the C_{60} vertical position, whereas the TBB network imposes the C_{60} lateral position, and stabilizes the molecule as well. The low charge density between the C_{60} and the SiB substrate on one hand, and on the other hand between the C_{60} and the TBB molecules, indicates that no covalent bond is formed between the C_{60} and its environment. However, according to charge density differences, a drastic charge reorganisation takes place between the Si adatoms and the C_{60} molecule, but also between the C_{60} and the surrounding TBB molecules. Finally, calculations show that a C_{60} array sandwiched between two TBB molecular layers is stable, which opens the way to the growth of 3D supramolecular networks.

1 Introduction

The outstanding properties of C_{60} molecules make them particularly promising in various domains such as nano-medicine[1,2] or nano-electronics[3]. Thus, one major challenge is to be able to control their growth and organisation. However, in C_{60} arrays, there is usually a competition between the C_{60}- substrate and the C_{60}- C_{60} interactions, which impedes the formation of long range ordered layers[4–7]. Moreover, the C_{60} molecules can interact strongly with the substrate, and consequently form covalent bonds[8–11], which means that the intrinsic C_{60} electronic properties are lost. A route has been open by depositing the C_{60} on a supramolecular network: the fullerene interacts with the network molecules, which reduces the C_{60} electronic coupling with the substrate[12,13]. In addition, the network separates the C_{60} molecules from each other, which decreases the intermolecular interactions[14,15], and thus favours their organisation. Many works are devoted to C_{60}/molecular networks deposit on metallic substrates, such as Au(111)[12,16], Ag(100)[17], Cu(110)[18], or Cu(100)[19]. If applications in nano-electronics are targeted, one needs a semi-conductor substrate, if possible cheap, such as silicon. Theobald *et al.* used a Si(111)-Ag $\sqrt{3}\times\sqrt{3}-R30^\circ$ surface on which perylene tetra-carboxylic di-imide and melamine was deposited, forming a honeycomb lattice[14]. The lattice parameter (34.6 Å) allowed to accommodate C_{60} heptamers within one nanopore. In the work[20] of Baris *et al.*, the substrate is a Si(111)$\sqrt{3}\times\sqrt{3}-R30^\circ$-B surface (hereafter referred to as SiB) where the B atom lies in S_5 position below a Si adatom. Thanks to boron doping, charge transfer between the Si adatoms and the B atoms depopulates the Si dangling bonds, leading to a SiB surface passivation[21–27]. On this surface the authors deposited 1,3,5-tri(1'-bromophenyl)benzene molecules (noted TBB), which form a supramolecular network[28]. Further deposition of C_{60} molecules results in the formation of an ordered array, where the C_{60} molecules are located within the nanopores formed by the TBB molecules[20]. The scanning tunnelling microscopy (STM) experimental and calculated images indicate that only one C_{60} molecule can be trapped in one nanopore. Here we present density functional theory (DFT) calculations performed on the C_{60} array organised on the TBB/SiB system. The van der Waals interactions are taken into account by using the semi-empirical correction of Grimme[29–31]. In particular we investigate the C_{60} adsorption energy as a function of the height of the molecule with respect to the SiB surface. It appears that the TBB molecules stabilize the fullerenes and define their lateral position on the surface. Subsequently, we studied the interactions between C_{60} and the substrate as well as between C_{60} and TBB molecules. We show that no covalent bonds are formed between C_{60} and its environment, but however that electrostatic-like and van der Waals interactions actually take place. Finally, we tested the stability of a second TBB layer added on top of the C_{60}/TBB/SiBB system. We find that the TBB/C_{60}/TBB/SiB system is stable, which opens the way to the growth of 3D supramoleculars frameworks.

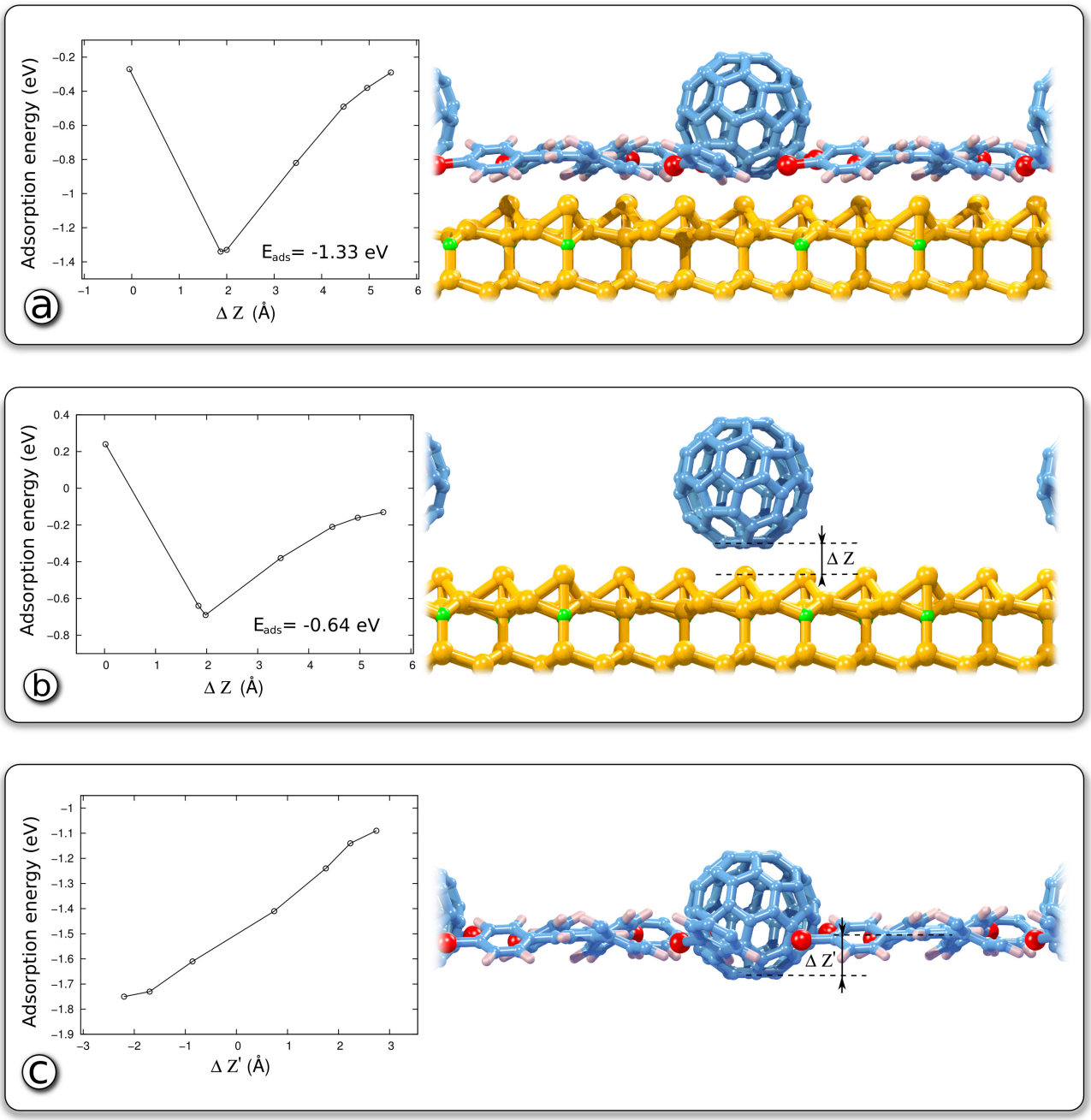

Fig. 1 Adsorption energy as a function of C_{60} height (left), along with ball-and-stick model (right, side-view) of the atomic structure for different relaxed systems. ΔZ corresponds to the height difference between the bottom C_{60} carbon atoms and the SiB substrate Si adatoms, while $\Delta Z'$, is related to the height difference between the bottom C_{60} carbon atoms and the plane defined by the TBB central phenyl rings, which are parallel to the SiB surface. (a) C_{60}/TBB/SiB; (b) C_{60}/SiB (c) C_{60}/TBB. The models present the C_{60} position corresponding to the lowest energy in the adsorption energy graphs. Carbon, bromine, silicon, boron, and hydrogen atoms are represented by blue, red, yellow, green, and pink colours, respectively.

2 Calculation details

The density functional theory (DFT) calculations are performed using the projector augmented plane-wave (PAW)[32,33] method in the framework of the Vienna ab-initio simulation package (VASP)[34,35]. The generalized gradient approximation of Perdew, Burke and Ernzerhof (PBE) is employed for the exchange-correlation potential[36]. A plane wave energy cutoff of 400 eV has been used for the calculations. Increasing the energy to 500 eV changes the C_{60} adsorption energy by only 0.02 eV. The dispersive interactions are taken into account by means of the DFT-D2 approach[29–31]. After the introduction of the van der Waals interaction in our simulations, no modification of the C_{60} densities of states has been noticed at a same atomic position. As the used supercell is large (20.1 $\AA \times 20.1$ $\AA \times 34$ $\AA$), the Brillouin zone is sampled using a single k-point at the Γ point. Increasing the number of k-points (from 1 to 14 irreducible k-points) modifies only slightly the calculated gap of the SiB slab (less than 0.05 eV). The ionic structure is relaxed until the components of the forces on each atom are less than 0.02 eV/$\AA$. The slab is defined as one layer of TBB molecules on top of five Si layers with B atoms at S_5 sites. H atoms are saturating the back-face Si bonds. One C_{60} is deposited on the previously defined slab. As a result, 288 atoms are necessary to compose the supercell. The SiB slab has already been successfully used for the study of the adsorption of an isolated Cu-5,10,15,20-tetrakis(3,5-di-tert-butyl-phenyl) porphyrin (Cu-TBPP)[37] and the adsorption of the TBB network[28]. The vacuum spacing is taken at about 16 $\AA$. The whole slab is allowed to relax except the H and bottom Si layers. The interactions between the C_{60} and the SiB or the molecular network are studied by means of a partial charge approach in the Bader scheme[38,39]. One indication of the quality of the Bader analysis results is the total number of valence electrons obtained from the integration over all the Bader regions (i.e. the conservation of charge). When using the $(196 \times 196 \times 336)$ grid, the total number of electrons is reproduced with an error lower than 4.10^{-4} e^-. We are able to conclude that the Bader charge is well converged with respect to the used mesh.

3 Results and Discussion

3.1 Energetic and structural study

The STM measurements of Baris *et al.*[20] have shown that the C_{60} molecules are located within the pores of the TBB network. In order to investigate the stability of the C_{60}, calculations were performed for a C_{60} molecule (presented in Fig.1a) positioned within the TBB nanopore, and centred on the triangle formed by three Si adatoms. The C_{60} hexagonal face, which is the densest one, is taken parallel to the substrate surface. The adsorption energy $E_{ads(C60onTBB/SiB)}$ is presented in Fig.1a as a function of the height of the C_{60} molecule, where

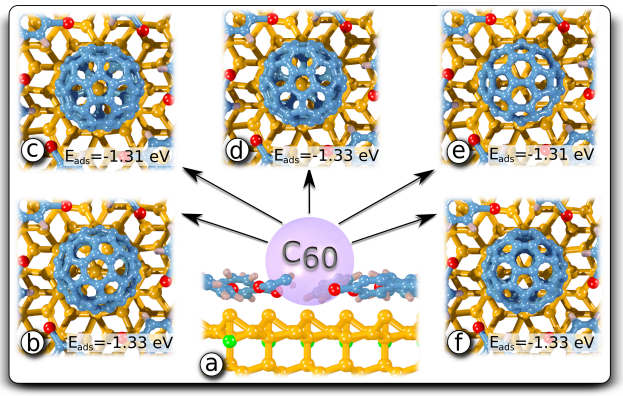

Fig. 2 Models for different C_{60} orientations within the TBB nanopore, along with related C_{60} adsorption energy. (*a*) general side view. Top views of the following orientations parallel to the surface: (*b*) hexagonal face, (*c*) pentagonal face, (*d*) 180 ° -rotated pentagonal face, (*e*) C-C bond between two hexagonal faces, (*f*) C-C bond between an hexagonal and a pentagonal face. Carbon, bromine, silicon, boron and hydrogen atoms are represented by blue, red, yellow, green and pink colours, respectively.

$$E_{ads(C60\ on\ TBB/SiB)} = E_{C60/TBB/SiB} - E_{TBB/SiB} - E_{isolated\ C60} \quad (1)$$

$E_{C60/TBB/SiB}$ is the total energy of the relaxed system, $E_{TBB/SiB}$ that of the relaxed supramolecular network on the SiB substrate, and $E_{isolated\ C60}$ represents the energy of the C60 molecule in gas phase.

When the C_{60} molecule approaches the TBB/SiB surface (Fig.1a), it appears that the adsorption energy decreases, and reaches a minimum value (-1.33 eV) when the height ΔZ between the bottom C atoms and the Si adatoms is 1.87 Å. When the molecule comes closer to the surface, the adsorption energy increases, due to repulsive interactions. Thus, the calculations indicate that the nanopore constitutes a stable position for the C_{60}.

In order to discriminate between the influence of the SiB substrate on the C_{60} molecules on one side, and of the TBB network on the other side, the adsorption energy has been calculated for two distinct models, namely the C_{60} molecules deposited on the bare SiB substrate (Fig.1b), and on the TBB network without the SiB substrate (Fig.1c). In Fig.1b, the C_{60} molecules are located at the same lateral positions as in Fig.1a (that is, above three Si adatoms), with a surface density of 1.11×10^{14} molecules *per* cm^2, identical to that of the TBB nanopores, arranged in a $3\sqrt{3} \times 3\sqrt{3}$ periodicity. The adsorption energy $E_{ads(C60\ on\ SiB)}$ is given by

$$E_{ads(C60\ on\ SiB)} = E_{C60/SiB} - E_{isolated\ C60} - E_{SiB} \quad (2)$$

$E_{C60/SiB}$ is the total energy of the relaxed system consisting of the SiB substrate with the C_{60} layer, while E_{SiB} is that of the bare relaxed SiB substrate. It can be seen in Fig.1b that, again, the adsorption energy diminishes when the C_{60}-SiB distance ΔZ decreases, and is minimum for a C_{60} height of 1.98 Å. It should be emphasized that the lowest adsorption energy for both the C_{60}/TBB/SiB and C_{60}/SiB systems corresponds to close vertical positions (1.87 Å and 1.98 Å respectively).

According to Fig.1, the minimum energy value for C_{60}/SiB is -0.64 eV, while that of the C_{60}/TBB/SiB system is -1.33 eV. These means that the molecular network tends to stabilize the C_{60} molecules. Thus we calculated the fullerene adsorption energy on the freestanding TBB network, as a function of the C_{60} height (Fig.1c). As the SiB support is absent, a new height reference has been chosen: $\Delta Z'$ corresponds to the height difference between the bottom carbon atoms of the C_{60} molecule and the TBB plane, defined by the TBB central phenyl rings. The adsorption energy has been calculated as

$$E_{ads(C60\ on\ TBB)} = E_{C60/TBB} - E_{TBB\ network} - E_{isolated\ C60} \quad (3)$$

Here $E_{TBB\ network}$ is the total energy of the unsupported relaxed molecular network. When the C_{60} molecule comes closer to the TBB network, the adsorption energy diminishes with lowering molecule height, as in both previous systems. However, because the SiB support is absent, and also the size of the nanopore (11 Å) is larger than the C_{60} covalent diameter (8 Å)[20], the fullerene is able to penetrate the TBB network. The adsorption energy keeps decreasing, at least till the height difference $\Delta Z'$ reaches -2.2 Å. The important point here is that the interaction between C_{60} and TBB molecules is not repulsive, and that the integration of the C_{60} within the TBB network is favoured. As a result, the adsorption energy of the C_{60} on top of the SiB support is lower (-1.33 eV versus -0.64 eV) when the TBB layer is present.

To summarize the information obtained from Fig.1b and 1c, we know that the TBB network does not limit the C_{60} height, but that the C_{60} interaction with the SiB substrate becomes repulsive when the molecule comes too close to the substrate. Then it can be concluded that it is the SiB substrate that governs the C_{60} height with respect to the surface.

However the C_{60} adsorption energy may depend on its orientation with respect to the surface, as has been shown on metals[40]. Thus we tested various C_{60} orientations by rotating the molecule within the nanopore (Fig.2a). We started from the hexagonal face parallel to the surface (Fig.2b), at the position giving the best adsorption energy in Fig.1a. In Fig.2c and 2d, the pentagonal face is taken parallel to the SiB support, with two azimuthal orientations with respect to the vertical axis, differing by 180°. Finally, in Fig.2e and 2f, a C-C bond is facing down, which is between two hexagonal faces, or an hexagonal and a pentagonal face, respectively. Clearly the adsorption energies are very close to each other, and the interactions between the fullerene and the SiB surface and TBB molecules do not depend on the C_{60} orientation (Fig.2). In the following, the hexagonal face parallel to the surface will be taken for the calculations.

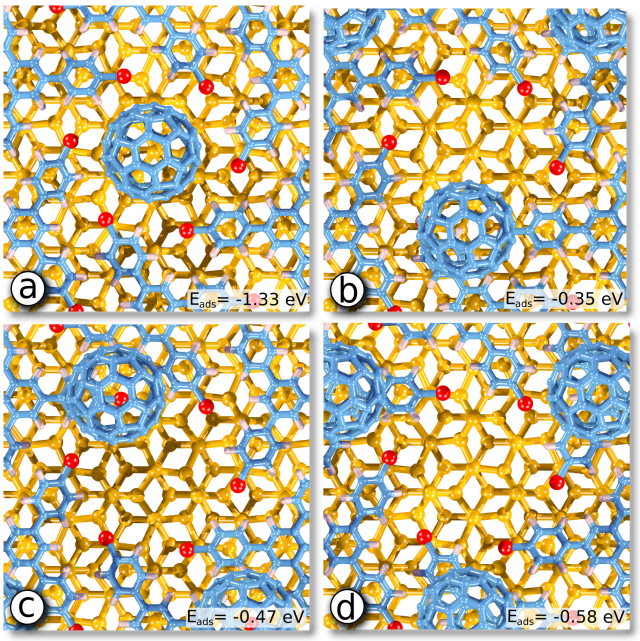

Fig. 3 Top view models for different C_{60} lateral positions with respect to the TBB network, along with related C_{60} adsorption energy. Carbon, bromine, silicon and hydrogen atoms are represented by blue, red, yellow and pink colours, respectively.

At this point the question is: why are the C_{60} molecules found experimentally only within the network nanopores, and not on top of the TBB molecules[20] ? To this aim, we tested the stability of different C_{60} lateral positions with respect to the molecular network. In Fig.3a, the C_{60} lies at the centre of the nanopore, as in Fig.1a. For Fig.3b the fullerene molecule is located between the adjacent Br atoms of two neighbouring TBB molecules, and in Fig.3c between two TBB molecules and above three Si adatoms. Finally, in Fig.3d, the C_{60} molecule is centred over the central phenyl ring of a TBB molecule. Fig.3 also displays the adsorption energy for each configuration. Clearly the lowest adsorption energy (-1.33 eV) corresponds to the C_{60} molecule surrounded by TBB molecules, and the C_{60} lateral position is imposed by the molecular network. In other words the nanopore is the most stable site, which is in agreement with the experimental data.

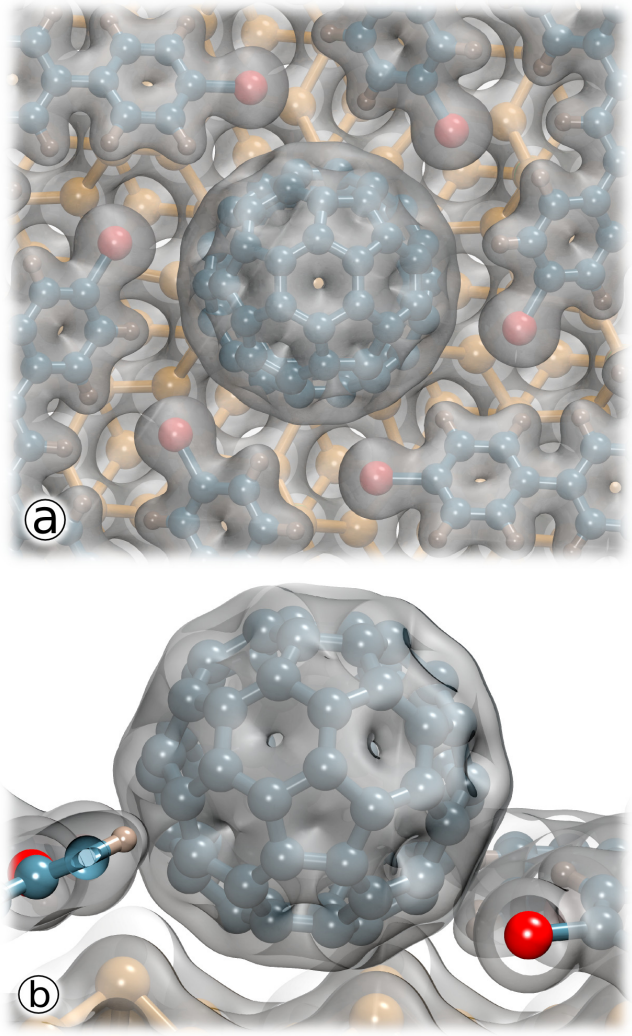

Fig. 4 Top and side views representing the total electron density (in translucent grey); the isodensity is equal to 0.2 $e^{-}/Å^{3}$. Carbon, bromine, silicon and hydrogen atoms are represented by blue, red, yellow and pink colours, respectively.

3.2 Electronic structure

The previous study has shown that the C_{60} interacts with both the TBB molecules and the SiB substrate. In order to be able to characterize these interactions, we present in Fig.4 density charge maps. At this charge density value ($0.2e^{-}/ Å^{3}$), the covalent bonds within the TBB or C_{60} molecules and the SiB substrate are visible. Nevertheless, no charges are present between the C_{60} and the TBB molecules (top view), or SiB substrate (side view). This means that the C_{60} does not share charges with the substrate or the surrounding molecules, and therefore that no bonds are formed between the fullerene molecule and its environment. This behaviour is very different from what can be observed for the deposition of C_{60} on a Si(111)-7×7 [8,10,11,41] or the SiC(0001)-3×3 surface [42]. Indeed for these systems the C_{60} molecules are chemisorbed by means of Si-C covalent bonds. It should be pointed out that the Si-C bond length in the C_{60}/Si(111) and C_{60}/SiC systems lies between 1.97 and 2.17 $Å$ [8,9,11,42], while for C_{60}/TBB/SiB the closest value for the Si-C distances between a C_{60} carbon atom and a Si adatom is 3.05 $Å$. This observation is in line with the absence of covalent bonds between the C_{60} and the SiB substrate.

However, according to the adsorption energy study, there is an attractive interaction between the C_{60} and the SiB surface, as well as with the TBB molecules. Note that in the case of C_{60} molecules deposited on bare SiB, the C_{60} grows initially at defects because of the presence of Si dangling bonds [27]. From these nucleation points, hexagonal close packed C_{60} domains can be obtained on the SiB terraces. At this stage the growth is driven by interactions between the C_{60} molecules, which are separated by a 1.18 nm distance. In contrast, when C_{60} is located in the nanopores of the TBB network, the distance between two fullerene molecules is about 2 nm, which is larger than on the bare SiB support. As a result, the interactions between C_{60} molecules are probably very weak, and the C_{60} growth is rather driven by the TBB network and the SiB substrate.

In order to get further understanding of the system, we performed charge differences maps as displayed in Fig.5. These data are obtained by calculating the difference between the charge density of the C_{60}/TBB/SiB relaxed system on one hand, and on the other hand the C_{60} isolated molecule and the TBB/SiB substrate taken at the atomic positions obtained previously (Fig.1a), without further atomic relaxation. A light green (lilac) zone corresponds to an augmentation (diminution) of the local electron density when bringing together the C_{60} molecule and the TBB/SiB substrate. In Fig.5a, 5b and 5c, one can observe a charge reorganisation mainly located along the axes between the C_{60} and the below lying Si adatoms. More precisely, the charge density diminishes above the Si adatoms, while it increases below the nearest C atoms in the

area between the C and Si atoms. These charge modifications are compensated around the Si adatoms (see the green half ring), and below the C atoms towards the bottom of the C_{60} molecules. This confirms that an interaction exists between the SiB surface and the C_{60} molecule, and indicates that it takes place between the C_{60} and the Si adatoms.

Now we have shown the presence of interactions mainly between the C_{60} and the Si adatoms of the SiB substrate. However the three green zones along the C_{60} in Fig.5b show that there is also a charge reorganisation between the C_{60} and the TBB molecules. Fig.5d and 5e display a side view and a top view map for a lower charge density difference than in Fig.5a and 5b. The top view (Fig.5e) indicates that three TBB molecules (for one C_{60}) are concerned by the charge modifications (let alone the slight electron gain on every Br atom). The charge increases at the C_{60} carbon atom nearest the TBB molecule, but also at a higher carbon atom bonded to the first one (see the side views in Fig.5a and 5d). This is related to the fact that the bromophenyl arm near the C_{60} is rotated upside. Note that there are three other bromophenyl arms located near the C_{60} molecule that do not undergo any charge reorganisation. This may be due to the fact that along this direction the interactions do not intervene between the TBB molecules and the C_{60}, but rather between the TBB and the Si adatoms, as the bromophenyl arms are now directed downside toward the Si adatoms[28].

In this respect, we calculated the Bader charges variation (table 1) for the different components of both the C_{60}/TBB/SiB and TBB/SiB systems. From the first column, it can be seen that charge is transferred to the C_{60} molecule (0.145 e^-). On the contrary, for C_{60}/Si(111), C-Si bonds are formed, and the charge transfer lies between 1 and 3 electrons[11,41,43,44]. In contrast, for systems displaying very weak interactions between the molecule and the substrate such as C_{60}/GaAs(100) or C_{60}/GaAs(110), the charge transfer is only 0.01 e^- or 0.02 e^- respectively[41,45,46]. Thus, the value of 0.145 e^- obtained here confirms the absence of covalent bonds between the C_{60} and the substrate or the molecular network. In addition, the TBB charge is also increased by 0.186 e^-. Note that the second column shows that this is not related to the presence of the C_{60}.

In order to obtain more informations on the influence of the SiB substrate and the TBB network on the C_{60} electronic structure, we calculated the C_{60} density of states (DOS) in gas phase and in the TBB/SiB nanopore. The data are presented in Fig.6 on the same graph for comparison. For the C_{60} in gas phase (solid line), well-defined peaks are observed. For the C_{60} in the nanopore (dashed line), the same features can also be found, which are shifted by 0.56 eV towards the lowest energies. This corresponds to an increased number of occupied levels, in agreement with the charge transfer to the C_{60} molecule obtained from Bader charges variation. Moreover, the peaks for the C_{60} in the nanopore present the same shape as in gas phase. In particular they are not widened or splitted, as has been observed for C_{60} molecules on Si(111)-7×7 or SiC(0001)-3×3 surfaces with the formation of covalent bonds[9,42]. Here the C_{60} keeps the characteristics of the isolated molecule, which confirms the absence of covalent bonds between the C_{60} and the SiB surface. As such, the C_{60}-SiB interactions are essentially electrostatic, whereas the interactions between the C_{60} and the TBB molecules are rather van der Waals ones.

Table 1 Bader charges variation (in e^- unit) for the different components in the C_{60}/TBB/SiB and TBB/SiB systems, with respect to the C_{60} and TBB in gas phase, and the bare SiB substrate.

	C_{60}/TBB/SiB	TBB/SiB
C_{60}	0.145	-
TBB	0.186	0.195
SiB	-0.331	-0.195

In the previous section, we have shown that deposition of C_{60} molecules on the TBB/SiB surface gives rise to marked charge reorganisations on the various species. Now we are going to investigate the stability of a second TBB monolayer deposited on top of the C_{60}/TBB/SiB previous system in order to built a 3*D* architecture. In this respect, P. Beton *et al.* successfully obtained a bilayer structure by adding C_{60} molecules to a p-terphenyl-1-3,5,3',5'-tetracarboxylic acid (TPTC) monolayer, previously deposited on a graphite HOPG substrate[47,48]. As a result, an ordered C_{60} array has been obtained sandwiched between two TPTC molecules layers. Fig.7 presents a side-view of the bilayer network obtained after relaxation. The C_{60} ordered array is now sandwiched between both TBB monolayers. The adsorption energy is defined as :

$$E_{ads(TBB\ on\ C60/TBB/SiB} = E_{TBB/C60/TBB/SiB} - E_{C60/TBB/SiB} - 2E_{isolated\ TBB} \quad (4)$$

where, $E_{TBB/C60/TBB/SiB}$ is the bilayer system total energy, $E_{C60/TBB/SiB}$ that of the system formed by the C_{60} array, the TBB network and the SiB substrate, and $E_{isolated\ TBB}$ corresponds to the energy of a TBB molecule in gas phase. The found value is $E_{ads(TBB\ on\ C60/TBB/SiB}$ = -3.71 eV, which is close to the adsorption energy of the first TBB layer on SiB (-3.44 eV)[28]. This result indicates that the bilayer system is stable. The distance between both layers is 3.72 Å, and the distance between the second TBB layer and the top of the C_{60} molecule is 1.84 Å. This value is larger than the distance between the first molecular layer and the bottom of the C_{60} molecule (0.93 Å). Indeed, because of the absence of the SiB substrate repulsive effect, the C_{60} molecule can deeper penetrate the TBB layer. As a matter of fact, the bromophenyl

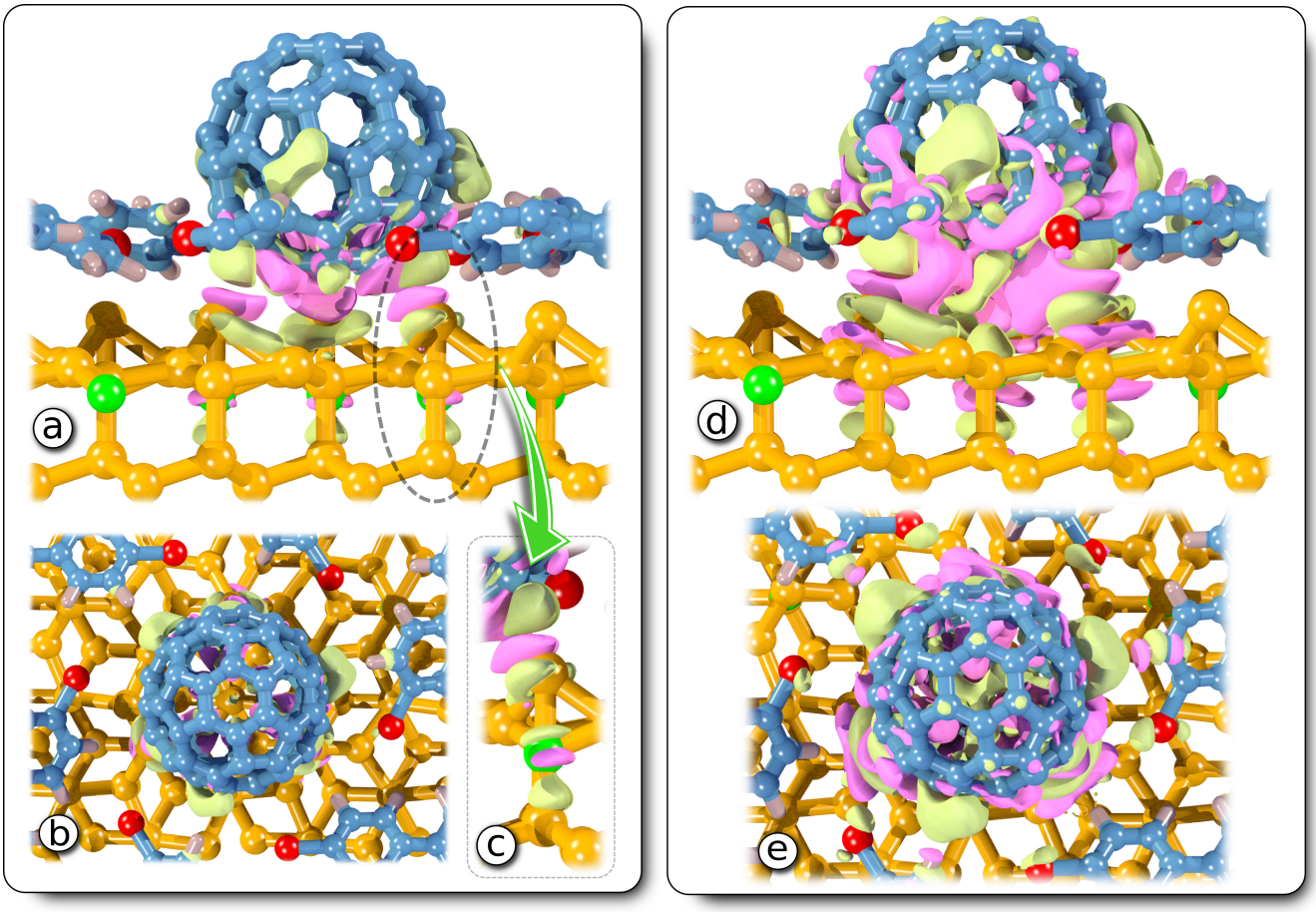

Fig. 5 Top and side views of the electron density difference induced by deposition of a C_{60} molecule in the nanopore of the TBB/SiB network. Light green and lilac plots correspond to augmentation and diminution of the local electron density, respectively. (a) , (b), (c) 0.002 $e^{-}/Å^3$; (d) , (e) 0.0008 $e^{-}/Å^3$. (c) presents an enlarged view of the zone marked with a dashed line in (a) where foreground Si atoms have been removed for clarity. Carbon, bromine, silicon, boron, and hydrogen atoms are represented by blue, red, yellow, green, and pink colours, respectively.

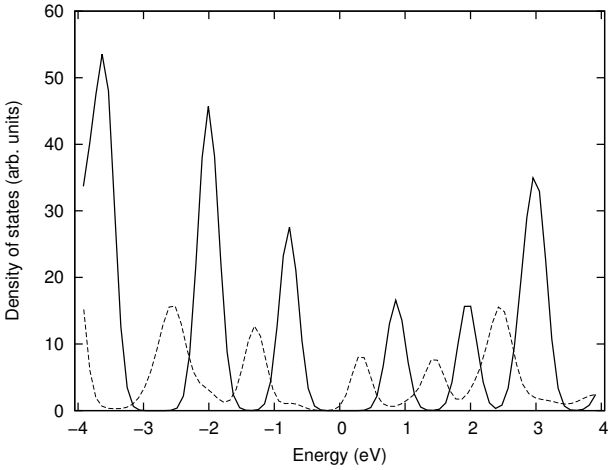

Fig. 6 Density of states as a function of energy of the C_{60} in gas phase (solid line) and of the C_{60} in the TBB/SiB nanopore (dashed line). The Fermi level is taken at 0 eV.

arms of the top TBB layer are rotated in a similar way to those belonging to the bottom layer, which favours the π stacking between parallel phenyl rings.

4 Conclusion

By means of DFT calculations, we have shown that the most stable position for C_{60} deposited onto a TBB/SiB supramolecular network is the centre of the nanopore formed by the TBB molecules. The SiB support controls the fullerene height, while the TBB molecules impose the lateral position. Charge density maps indicate that no covalent bonds are formed between the C_{60} carbon atoms and either the Si substrate atoms, or the TBB molecules. Nevertheless a drastic charge reorganisation takes place at the C_{60} and TBB molecules, and at the Si adatoms, which means that the C_{60} clearly interacts with its environment. Finally, we found that a second TBB organised overlayer can be stabilized on top of the C_{60}/TBB/SiB system. Contrary to the TPTC/C_{60}/TPTC bilayer obtained by Beton *et al.*, where the C_{60} array cannot be observed independently from the top molecular layer, here we propose a new process to obtain a 3*D* molecular architecture. It consists of a controlled step by step construction, where the TBB molecular network is first realised[28], followed by C_{60} molecules deposition[20]. Our calculations show that the final step - namely the growth of a second TBB molecular network - can be considered. This three-dimensional architecture, which is challenging from both the experimental and theoretical point of views, deserves to be investigated thoroughly, as it opens the way to new perspectives for the growth of supramolecular networks.

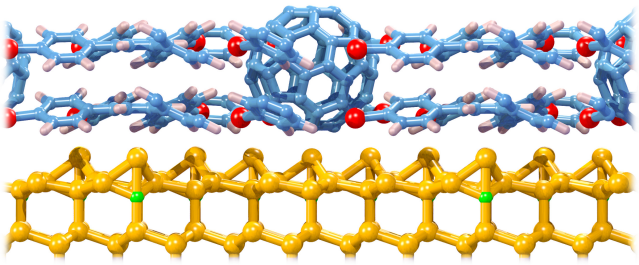

Fig. 7 Side view of the TBB/C_{60}/TBB/SiB relaxed atomic structure. Carbon, bromine, silicon, boron, and hydrogen atoms are represented by blue, red, yellow, green, and pink balls, respectively.

5 Acknowledgments

This work was performed using HPC resources from GENCI-IDRIS (grant 2012-092042) and the supercomputer facilities of the Mésocentre de calcul de Franche-Comté. The French Agency ANR (ANR-09-NANO-038) has supported this work.

References

1 J. Barnoud, G. Rossi and L. Monticelli, *Phys. Rev. Lett.*, 2014, **112**, 068102.
2 R. Bakry, R. Vallant, M. Najam-Ul-Haq, M. Rainer, Z. Szabo, C. Huck and G. Bonn, *Int. J. Nanomedicine*, 2007, **130**, 639–649.
3 H. Park, J. Park, A. K. L. Lim, E. H. Anderson, A. P. Alivisatos and P. L. McEuen, *Nature*, 2000, **407**, 57.
4 D. Olyanich, T. Utas, V. Kotlyar, A. Zotov, A. Saranin, L. Romashev, N. Solin and V. Ustinov, *Appl. Surf. Sci.*, 2014, **292**, 954 – 957.
5 D. Gruznev, A. Matetskiy, I. Gvozd, A. Zotov and A. Saranin, *Surf. Sci.*, 2011, **605**, 1951 – 1955.
6 M. D. Upward, P. Moriarty and P. H. Beton, *Phys. Rev. B*, 1997, **56**, R1704–R1707.
7 T. Nakayama, J. Onoe, K. Takeuchi and M. Aono, *Phys. Rev. B*, 1999, **59**, 12627–12631.
8 R. Rurali, R. Cuadrado and J. I. Cerdá, *Phys. Rev. B*, 2010, **81**, 075419.
9 J. Y. Lee and M. H. Kang, *Surf. Sci.*, 2008, **602**, 1408–1412.
10 S. Gangopadhyay, R. Woolley, R. Danza, M. Phillips, K. Schulte, L. Wang, V. Dhanak and P. Moriarty, *Surf. Sci.*, 2009, **603**, 2896 – 2901.
11 D. Sánchez-Portal, E. Artacho, J. I. Pascual, J. Gómez-Herrero, R. M. Martin and J. M. Soler, *Surf. Sci.*, 2001, **482-485**, 39–43.
12 K. J. Franke, G. Schulze, N. Henningsen, I. Fernández-Torrente, J. I. Pascual, S. Zarwell, K. Rück-Braun, M. Cobian and N. Lorente, *Phys. Rev. Lett.*, 2008, **100**, 036807.
13 G.-B. Pan, X.-H. Cheng, S. Coger and W. Freyland, *J. Am. Chem. Soc.*, 2006, **128**, 4218.
14 J. Theobald, N. Oxtoby, M. Phillips, N. Champness and P. Beton, *Nature*, 2003, **424**, 1029.
15 L. Sánchez, R. Otero, J. M. Gallego, R. Miranda and N. Martín, *Chem. Rev.*, 2009, **109**, 2081–2091.
16 S. Yoshimoto, Y. Honda, O. Ito and K. Itaya, *J. Am. Chem. Soc.*, 2008, **130**, 1085–1092.
17 D. Bonifazi, H. Spillmann, A. Kiebele, M. de Wild, P. Seiler, F. Cheng, H.-J. Güntherodt, T. Jung and F. Diederich, *Angew. Chem. Int. Ed.*, 2004, **43**, 4759.
18 W. Xiao, D. Passerone, P. Ruffieux, K. AïtMansour, O. Gröning,

E. Tosatti, J. S. Siegel and R. Fasel, *J. Am. Chem. Soc.*, 2008, **130**, 4767–4771.
19 S. Stepanow, M. Lingenfelder, A. Dmitriev, H. Spillmann, E. Delvigne, N. Lin, X. Deng, C. Cai, J. V. Barth and K. Kern, *Nat. Mater.*, 2004, **3**, 229.
20 B. Baris, V. Luzet, E. Duverger, P. Sonnet, F. Palmino and F. Cherioux, *Angew. Chem.*, 2011, **50**, 4094–4098.
21 P. Bedrossian, R. D. Meade, K. Mortensen, D. M. Chen, J. A. Golovchenko and D. Vanderbilt, *Phys. Rev. Lett.*, 1989, **63**, 1257–1260.
22 I.-W. Lyo, E. Kaxiras and P. Avouris, *Phys. Rev. Lett.*, 1989, **63**, 1261–1264.
23 E. Kaxiras, K. C. Pandey, F. J. Himpsel and R. M. Tromp, *Phys. Rev. B*, 1990, **41**, 1262–1265.
24 M. R. H. Shi and P. Smith, *Sur. Rev. and Lett.*, 2003, **10**, 201.
25 T. Stimpel, J. Schulze, H. Hoster, I. Eisele and H. Baumgrtner, *Appl. Surf. Sci.*, 2000, **162163**, 384–389.
26 W. Mönch, in *Semiconductor Surfaces and Interfaces*, Springer Berlin Heidelberg, 1993, vol. 26, pp. 257–264.
27 T. Stimpel, M. Schraufstetter, H. Baumgrtner and I. Eisele, *Mater. Sci. Eng. : B*, 2002, **89**, 394 – 398.
28 K. Boukari, E. Duverger and P. Sonnet, *J. Chem Phys.*, 2013, **138**, 084704.
29 S. Grimme, *J. Comput. Chem.*, 2006, **27**, 1787–1799.
30 S. Grimme, *J. Comput. Chem.*, 2004, **25**, 1463–1473.
31 S. Grimme, J. Antony, T. Schwabe and C. Mück-Lichtenfeld, *Org. Biomol. Chem.*, 2007, **5**, 741.
32 P. E. Blöchl, *Phys. Rev. B*, 1994, **50**, 17953.
33 G. Kresse and J. Furthmüller, *Phys. Rev. B*, 1996, **54**, 11169.
34 G. Kresse and D. Joubert, *Phys. Rev. B*, 1999, **59**, 1758.
35 G. Kresse and J. Hafner, *Phys. Rev. B*, 1994, **49**, 14251.
36 J. P. Perdew, K. Burke and M. Ernzerhof, *Phys. Rev. Lett.*, 1996, **77**, 3865.
37 K. Boukari, P. Sonnet and E. Duverger, *ChemPhysChem*, 2012, **13**, 3945.
38 R. F. W. Bader, *Chem. Rev.*, 1991, **91**, 893–928.
39 G. Henkelman, A. Arnaldsson and H. Jónsson, *Comput. Mater. Sci.*, 2006, **36**, 354 – 360.
40 K. Pussi, H. I. Li, H. Shin, L. N. Serkovic Loli, A. K. Shukla, J. Ledieu, V. Fournee, L. L. Wang, S. Y. Su, K. E. Marino, M. V. Snyder and R. D. Diehl, *Phys. Rev. B*, 2012, **86**, 205406.
41 P. Moriarty, *Surf. Sci. Rep.*, 2010, **65**, 175–227.
42 T. Ovramenko, F. Spillebout, F. C. Bocquet, A. J. Mayne, G. Dujardin, P. Sonnet, L. Stauffer, Y. Ksari and J.-M. Themlin, *Phys. Rev. B*, 2013, **87**, 155421.
43 S. Suto, A. Kasuya, O. Ikeno, C.-W. Hu, A. Wawro, R. Nishitani and R. Goto, *Jpn. J. Appl. Phys*, 1994, **33**, L1489–L1492.
44 T. Yamaguchi and S. Miyoshi, *Surf. Sci.*, 1996, **357-358**, 283–288.
45 A. Brambilla, P. Sessi, L. Duo, M. Finazzi, J. Cabanillas-Gonzalez, H.-J. Egelhaaf, G. Lanzani and F. Ciccacci, *Surf. Sci.*, 2007, **601**, 4078–4081.
46 T. R. Ohno, Y. Chen, S. E. Harvey, G. H. Kroll, J. H. Weaver, R. E. Haufler and R. E. Smalley, *Phys. Rev. B*, 1991, **44**, 13747–13755.
47 M. O. Blunt, J. C. Russell, G.-L. del Carmen, N. Taleb, X. Lin, M. Schröder, N. R. Champness and P. H. Beton, *Nat. Chem.*, 2011, **3**, 74.
48 S. De Feyter, *Nat. Chem.*, 2011, **3**, 14.